Spectrum of disease outcomes in mice infected with YFV-17D

Andrea K. Erickson and Julie K. Pfeiffer

Department of Microbiology, University of Texas Southwestern Medical Center,
5323 Harry Hines Blvd, Dallas, TX 75390-9048, USA

Correspondence
Julie K. Pfeiffer
Julie.Pfeiffer@UTSouthwestern.edu

The host and viral factors that influence disease outcome during flavivirus infections are not fully understood. Using the live attenuated yellow fever virus (YFV) vaccine strain 17D as a model system we evaluated how viral dose, inoculation route and immunopathogenesis contributed to disease outcome in mice deficient in the type I IFN response. We found that YFV-17D infection of IFN-α/β receptor knockout mice resulted in three distinct disease outcomes: no clinical signs of disease, fatal viscerotropic disease or fatal neurotropic disease. Interestingly, viral load at disease onset did not correlate with disease outcome. However, we found increased immune infiltrates in the brain tissues of mice that developed neurotropic disease. Additionally, mice that developed viscerotropic disease, as characterized by liver and spleen pathology and/or intestinal haemorrhage, had significantly elevated levels of alanine aminotransferase, monocyte chemotactic protein and IFN-inducible protein (IP)-10 as compared with mice with no clinical signs of disease or neurotropic disease. Furthermore, mice treated with recombinant IP-10 throughout YFV-17D infection showed increased mortality and an increased percentage of mice with viscerotropic disease. Our results demonstrated that viral load did not correlate with pathogenesis, and the host immune response played a pivotal role in disease outcome and contributed to YFV-17D pathogenesis in mice.

INTRODUCTION

Viral infection can cause a spectrum of disease phenotypes, ranging from severe fatal disease to asymptomatic infection. Infection with some viruses damages very specific sites, whilst infection with other viruses damages multiple body sites. Factors that influence different disease phenotypes are unclear. The goal of this study was to examine factors that contribute to distinct disease phenotypes using a mouse infection model.

Yellow fever virus (YFV) is the prototypical member of the genus *Flavivirus*, which includes other mosquito-borne human pathogens such as *dengue virus* (DENV), *West Nile virus* (WNV) and *Japanese encephalitis virus* (JEV). Despite the availability of vaccine and mosquito control pro-grammes, YFV is considered a re-emerging disease with ~200 000 new cases and ~30 000 deaths estimated each year. Yellow fever disease in humans can range from asympto-matic to severe haemorrhagic fever. Approximately 20 % of YFV-infected individuals develop a severe visceral disease involving many organs, particularly the liver. Fatal YFV infection is induced by systemic shock and multi-organ failure, and immunopathology or 'cytokine storm' correlates with disease severity (Monath, 2008; Monath & Barrett,

2003; ter Meulen *et al.*, 2004). Elevated levels of IL-6, IL-1 receptor antagonist, TNF-α, IFN-inducible protein (IP)-10 and monocyte chemotactic protein (MCP)-1 were found in patients with fatal YFV infection (ter Meulen *et al.*, 2004).

The YFV-17D vaccine is a live attenuated virus derived from the pathogenic Asibi strain of YFV. Although undeniably one of the safest live attenuated vaccines in history, rare severe adverse events can occur. These vaccine-associated adverse events are categorized as either YFV-17D-associated neurotropic disease (YFV-AND) or YFV-17D-associated viscerotropic disease (YFV-AVD). Encephalitis with fever and variable neurological signs are characteristic of YFV-AND, which typically resolve completely. However, a few YFV-AND cases have been fatal with virus recovered from brain tissues and the YFV-17D genome detected in the cerebral spinal fluid (Anonymous,1966; Kengsakul *et al.*, 2002; Monath *et al.*, 2013). The pathogenesis of YFV-AVD is similar to severe WT YFV infection with high case-fatality rates characterized by viral replication in numerous visceral tissues and liver histopathology (Belsher *et al.*, 2007; Centers for Disease Control and Prevention, 2002; Cetron *et al.*, 2002; Chan *et al.*, 2001; Gerasimon & Lowry, 2005; Martin *et al.*, 2001; Monath *et al.*, 2013; Vasconcelos *et al.*, 2001). Evaluation of the immune response in a few cases of YFV-17D-associated adverse events found elevated levels of liver enzymes and cytokines similar to WT YFV infection (Bae

et al., 2008; Silva *et al.*, 2010). It has been shown that YFV-17D can infect monocytes/macrophages and endothelial cells (Goodman & Koprowski, 1962; Khaiboullina *et al.*, 2005; Liprandi & Walder, 1983; Meier *et al.*, 2009; Schlesinger & Brandriss, 1981), and it has been proposed that these cells are a source of dysregulated cytokine secretion leading to sepsis (Khaiboullina *et al.*, 2005; Monath & Barrett, 2003). Whilst these YFV-17D-associated adverse events are rare, they can be quite serious. Therefore, a clearer understanding of the pathogenesis of YFV and YFV-17D is needed.

Although the YFV-17D vaccine is highly efficacious and has been in use since the 1930s, the molecular determinants and *in vivo* mechanisms for virulence attenuation are not fully understood. Attenuation of YFV-17D has been attributed to mutations in the YFV-17D envelope protein, which may hinder spread of the virus to visceral tissues, and was recently linked to reduced quasispecies diversity (Beck *et al.*, 2014; Hahn *et al.*, 1987; Lee & Lobigs, 2008). Considering that YFV-17D is currently being used in chimeric vaccines to JEV, and for the development of vaccines to WNV and DENV, a better understanding of its attenuation is imperative (Guirakhoo *et al.*, 2006; Guy *et al.*, 2010; Monath *et al.*, 2003, 2006; Pugachev *et al.*, 2005).

Laboratory rodents have varying degrees of susceptibility to YFV and YFV-17D infection, with disease outcome dependent on age, viral strain, immune status of the host, inoculation route and viral inoculum titre (Barrett & Gould, 1986; Fitzgeorge & Bradish, 1980; Horsfall, 1965; Lee & Lobigs, 2008; Meier *et al.*, 2009; Theiler, 1930; Thibodeaux *et al.*, 2012; Zisman *et al.*, 1971). Infant mice are susceptible to fatal infection with intravenously or intraperitoneally injected virulent strains of YFV, including YFV-Asibi, as well as attenuated strains of YFV, such as YFV-17D (Fitzgeorge & Bradish, 1980; Horsfall, 1965; Zisman *et al.*, 1971). However, immune-competent adult mice are not susceptible to lethal infection delivered by peripheral injection, but are susceptible following intracerebral injection with virulent or attenuated YFV (Fitzgeorge & Bradish, 1980; Fox, 1943; Goodman & Koprowski, 1962; Sellards, 1931; Theiler, 1930). In these cases, mice develop YFV-induced encephalitis regardless of viral strain. YFV can cause a viscerotropic disease resembling human disease, but only in peripherally injected immunodeficient animals such as mice deficient for IFN-α/β receptors (Meier *et al.*, 2009). Peripheral injection of YFV-17D in adult mice lacking both IFN-α/β receptors and IFN-γ receptors can cause a lethal neurotropic infection with transient viral infection of visceral organs and no observed tissue damage (Meier *et al.*, 2009; Lee & Lobigs, 2008; Thibodeaux *et al.*, 2012). Using a genetically marked pool of viruses, we previously found that YFV-17D encounters no major barriers that restrict viral diversity or dissemination in mice that lack IFN-α/β receptors (Erickson & Pfeiffer, 2013).

In the current study, we investigated how viral dose, inoculation route and the host immune response contributed to pathogenesis of YFV-17D in immune-competent C57BL/6 mice (IFNAR$^{+/+}$) and immune-deficient C57BL/6 mice lacking IFN-α/β receptors (IFNAR$^{-/-}$). We found that YFV-17D was severely attenuated in immune-competent mice regardless of route or viral dose and no mice exhibited clinical signs of disease. In contrast, after peripheral inoculation, YFV-17D rapidly disseminated in IFNAR$^{-/-}$ mice causing three distinct disease phenotypes: no clinical signs of disease, fatal viscerotropic disease or fatal neurological disease. Surprisingly, viral titres in various tissues at disease onset did not correlate with disease outcome. However, we found increased immune infiltrates in the brains of mice with neurotropic disease and increased cytokine levels (MCP-1 and IP-10) in mice with viscerotropic disease. Furthermore, we demonstrated that treatment with exogenous IP-10 increased YFV-17D pathogenesis in immune-deficient mice with significantly more mice succumbing to viscerotropic disease. Our results suggested that immunopathology likely contributed to the development of the three distinct disease phenotypes in YFV-17D-inoculated IFNAR$^{-/-}$ mice.

RESULTS

Inoculation route influences YFV-17D pathogenesis in IFNAR$^{-/-}$ mice

In order to evaluate YFV-17D pathogenesis we inoculated 3–4-week-old IFNAR$^{+/+}$ or IFNAR$^{-/-}$ mice intramuscularly, intraperitoneally, subcutaneously or in the footpad with 10^4 p.f.u. YFV-17D virus and monitored animals daily for signs of disease. We found that regardless of inoculation route, immune-competent mice did not exhibit signs of disease up to 30 days post-infection (p.i.) (Fig. 1a). Whilst footpad-inoculated IFNAR$^{-/-}$ mice had transient swelling at the site of inoculation, these animals fully recovered by 6 days p.i. Additionally, IFNAR$^{-/-}$ mice inoculated subcutaneously displayed no signs of disease at any point after infection.

In contrast, YFV-17D intramuscularly inoculated IFNAR$^{-/-}$ mice displayed varying degrees of illness. At 5 days p.i., all intramuscularly inoculated mice were limping on the injected leg; however, by 6 days p.i. the mice were walking normally. At 7–8 days p.i., 32 % of the intramuscularly inoculated IFNAR$^{-/-}$ mice presented with one of two disease phenotypes: neurotropic disease or viscerotropic disease (Fig. 1b). Neurotropic disease manifested as paralysis ranging from one paralysed leg to severe hind-limb paralysis. Viscerotropic disease manifested as lethargy, hunched posture, ruffled fur and rapid breathing. Whilst neurotropic disease onset was slow and progressed over a 24–48 h window, viscerotropic disease onset was rapid and progressed over just a few hours. In fact, 9 % of animals with viscerotropic disease were found dead within 12 h of appearing healthy (Table 1). Additionally, 91 % of mice with viscerotropic disease had damage to visceral organs: 23 % had splenomegaly (spleen length >1.5 cm; Fig. 1c), 14 % had liver pathology (Fig. 1d) and 54 % had intestinal
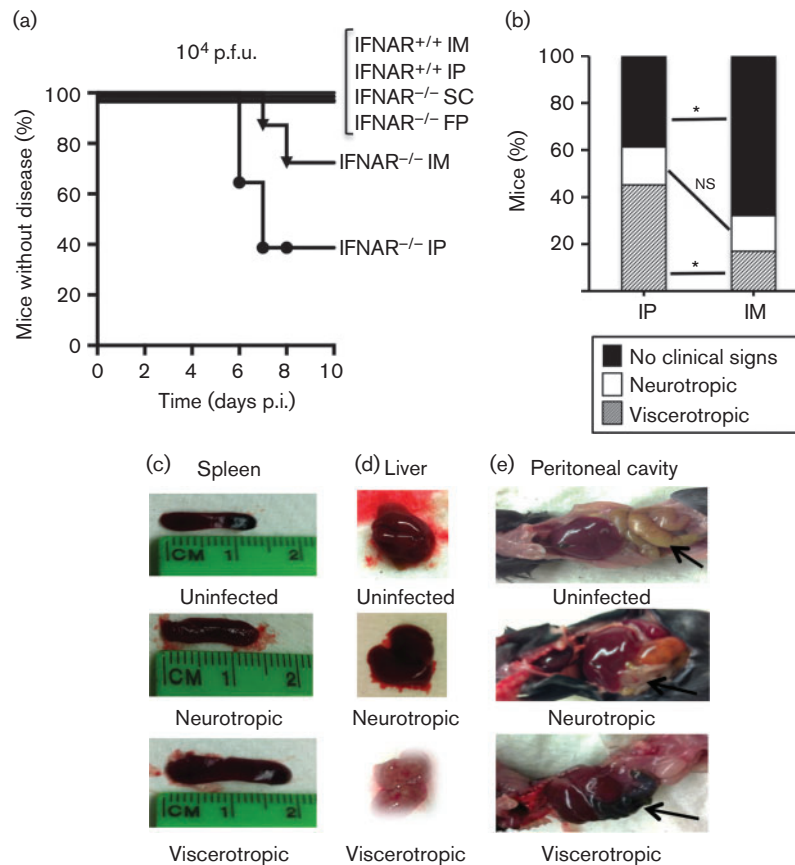
Fig. 1. Pathogenesis of YFV-17D infection in mice. (a) Survival of YFV-17D-infected mice. Mice (3–4 weeks old) were injected intramuscularly (IM), intraperitoneally (IP), subcutaneously (SC) or in the footpad (FP) with 10^4 p.f.u. YFV-17D and disease onset was monitored. As moribund mice do not recover from infection, they were euthanized upon severe disease onset; therefore, data are shown as the percentage without disease. Data are from three to six mice per condition for IFNAR$^{+/+}$ (intramuscular or intraperitoneal) and IFNAR$^{-/-}$ (subcutaneous or footpad). Data are from 31–53 mice per condition for IFNAR$^{-/-}$ (intraperitoneal or intramuscular). Statistically significant differences between conditions were found for the following: IFNAR$^{-/-}$ intramuscular versus intraperitoneal and IFNAR$^{-/-}$ intramuscular and intraperitoneal versus all other conditions ($P<0.005$, Mantel−Cox test). (b) Percentages of mice displaying no clinical signs of disease, neurotropic disease or viscerotropic disease according to inoculation route. Data were derived from 53 intramuscularly inoculated or 31 intraperitoneally inoculated IFNAR$^{-/-}$ mice. Statistically significant differences in the percentage of mice developing viscerotropic disease ($P<0.0001$, χ^2 test) and no signs of disease ($P=0.006$, χ^2 test) existed for intramuscularly versus intraperitoneally injected mice as indicated by asterisks. NS, Not significant. (c) Spleen pathology, (d) liver pathology and (e) visceral pathology in the peritoneal cavity, with arrows indicating the intestine; tissues were harvested from IFNAR$^{-/-}$ mice upon disease onset or from uninfected mice.

haemorrhage (Fig. 1e, arrows) (Table 1). Spleen, liver and intestine from mice with neurotropic disease or mice with no clinical signs appeared normal, similar to uninfected animals (Fig. 1c–e). All mice that survived through day 8 p.i. recovered completely, showing no signs of disease through 30 days p.i., regardless of inoculation route.

YFV-17D intraperitoneally inoculated IFNAR$^{-/-}$ mice displayed disease phenotypes similar to intramuscularly inoculated IFNAR$^{-/-}$ mice, but had significantly increased mortality, with 61 % of animals succumbing to infection at 6–7 days p.i. (Fig. 1a). Furthermore, we found that inoculation route influenced disease outcome, with viscerotropic disease developing in 45 % of intraperitoneally inoculated

IFNAR$^{-/-}$ mice compared with 17 % of intramuscularly inoculated IFNAR$^{-/-}$ mice (Fig. 1b). These results demonstrated that inoculation route influenced YFV-17D pathogenesis in IFNAR$^{-/-}$ mice.

Effect of viral dose and host age on YFV-17D pathogenesis in IFNAR$^{-/-}$ mice

To determine whether viral dose or host age affected YFV-17D pathogenesis, we examined disease outcome in mice inoculated with 1000-fold more virus and in older mice. First, we intramuscularly inoculated 3–4-week-old IFNAR$^{+/+}$ and IFNAR$^{-/-}$ mice with 10^7 p.f.u. YFV-17D virus and

Table 1. Characteristics of disease phenotypes in intramuscularly injected YFV-17D-infected mice

Characteristic	No clinical signs	Viscerotropic	Neurotropic
Disease manifestation			
Found dead (%)*	0	9	0
Lethargic/hunched (%)	0	91	0
Paralysis (%)	0	0	100
Tissue pathology			
Liver pathology (%)	0	14	0
Splenomegaly (%)	0	23	0
Intestinal haemorrhage (%)	0	54	0
Immune infiltrate in brain‡	−/−	+/−	+/+
Viral titre†			
Brain	+	+	+
Muscle	+/−	+	+/−
Blood	−	+/−	+/−
Liver	−	+/−	+/−
Spleen	−	+	+/−

*Mice were checked every 12 h. Therefore, mice that were found dead had appeared healthy $\leqslant 12$ h prior to their death, indicating rapid disease progression.

†Viral titres were undetectable (−), variable (+/−, undetectable to $\sim 10^5$ p.f.u.) or high (+, $>10^3$ p.f.u./tissue).

‡Immune infiltrate in brain was scored as high (+/+), medium (+/−), or low (−/−) according to data shown in Figure 4.

monitored animals daily for signs of disease. We found that none of the immune-competent mice displayed signs of disease, whilst 42 % of IFNAR$^{-/-}$ mice developed disease (Fig. 2a). Similar to results from IFNAR$^{-/-}$ mice inoculated with 10^4 p.f.u. YFV-17D by the intramuscular route, mice inoculated with 10^7 p.f.u. by the intramuscular route had similar percentages of mice developing viscerotropic or neurotropic disease (Figs 1b and 2b). Therefore, mice inoculated with 1000-fold more YFV-17D had only slightly higher mortality (42 versus 32 %; $P=0.15$, Mantel–Cox test) and the ratio of viscerotropic to neurotropic disease was unchanged. Additionally, we intramuscularly inoculated 6–7-week-old IFNAR$^{-/-}$ mice with 10^7 p.f.u. YFV-17D virus and monitored animals daily for signs of disease. We found that none of the older mice displayed signs of disease up to 21 days p.i. (data not shown). Taken together, these results demonstrated that increasing the viral inoculum 1000-fold did not significantly alter mortality or the percentage of mice with neurotropic or viscerotropic disease outcome.

YFV-17D titres in IFNAR$^{-/-}$ mice

To determine whether YFV-17D pathogenesis and disease outcome in IFNAR$^{-/-}$ mice correlated with viral titre, we inoculated mice intramuscularly or intraperitoneally with 10^4 p.f.u. YFV-17D, and at disease onset, or 8 days p.i. for mice with no clinical signs of disease, we harvested numerous tissues and evaluated viral loads by titre assay. We compared titres from leg muscle, sciatic nerve, blood, liver, spleen and brain in mice showing no clinical signs of disease, viscerotropic disease or neurotropic disease (Fig. 3). Regardless of disease state, we found high viral loads in the muscle of most intramuscularly inoculated IFNAR$^{-/-}$ mice, which was not surprising as muscle was the inoculation

site (Fig. 3a). However, >75 % of intraperitoneally inoculated mice with viscerotropic disease had detectable viral loads in muscle, suggesting viral dissemination from the peritoneal cavity (Fig. 3b). In contrast, viral titres were low or undetectable at 8 days p.i. in muscle tissues of intramuscularly or intraperitoneally inoculated IFNAR$^{+/+}$ mice (data not shown). These results suggested that, as expected, the type I IFN response limited YFV-17D replication in mice. Perhaps not surprisingly, mice with viscerotropic disease had higher viral titres in visceral tissues, such as spleen and liver, compared with mice showing no clinical signs of disease (Fig. 3a). However, there were no significant differences in visceral tissue titres in mice with viscerotropic versus neurotropic disease regardless of inoculation route (Fig. 3).

Previous studies have shown that neurotropic viruses can initiate infection in the periphery and can move through peripheral neurons to reach the central nervous system (Card *et al.*, 1991; Ohka *et al.*, 1998; Samuel *et al.*, 2007; Tyler *et al.*, 1986). Therefore, we hypothesized that mice with neurotropic disease may have higher viral titres in peripheral neurons and brain. We quantified viral titres in the sciatic nerve of YFV-17D-infected IFNAR$^{-/-}$ mice and found 10- to 100-fold higher viral titres in mice with disease as compared with mice with no clinical signs of disease (Fig. 3). Surprisingly, sciatic nerve titres and brain titres were not significantly higher in mice with neurotropic disease versus mice with viscerotropic disease. In fact, mice with viscerotropic disease had the highest brain titres regardless of inoculation route. Furthermore, mice showing no clinical signs of disease routinely had $>10^4$ p.f.u. in the brain at 8 days p.i. (Fig. 3), although viral titres in the brain were undetectable by 21 days p.i. (data not shown). Taken together, these results suggested that viral load did not necessarily correlate with disease.
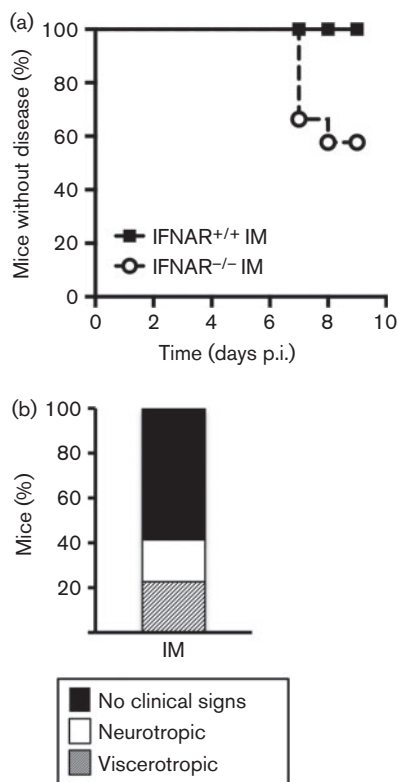
Fig. 2. Pathogenesis of YFV-17D infection in mice using a high viral inoculum. (a) Survival of mice infected with 10^7 p.f.u. YFV-17D. Mice (3–4 weeks old) were injected intramuscularly (IM) with 10^7 p.f.u. YFV-17D and disease onset was monitored. Data are shown as the percentage without disease. Data were from 26 IFNAR$^{+/+}$ and 128 IFNAR$^{-/-}$ mice. Statistically significant differences between IFNAR$^{+/+}$ and IFNAR$^{-/-}$ pathogenesis were observed ($P<0.0001$, Mantel–Cox test). However, there was no statistically significant difference in survival for IFNAR$^{-/-}$ mice injected intramuscularly with 10^4 versus 10^7 p.f.u. YFV-17D ($P=0.15$, Mantel–Cox test). (b) Percentages of mice displaying no clinical signs of disease, neurotropic disease or viscerotropic disease.

Mice with YFV-17D neurotropic disease have immune cell infiltrates in the brain

Considering that mice with no clinical signs of disease had $>10^4$ p.f.u. virus in brain tissue, we hypothesized that viral load alone was not inducing disease and that perhaps the immune response contributed to pathogenesis. In order to evaluate the presence of inflammatory cell infiltrates, hippocampal brain sections from uninfected and YFV-17D-infected IFNAR$^{-/-}$ mice were histologically stained with haematoxylin and eosin (HE) at 8 days p.i. We compared sections from uninfected mice with sections from infected mice displaying no clinical signs of disease, neurotropic disease or viscerotropic disease. We found that brain sections from YFV-17D-infected mice showing no clinical signs of disease were very similar to uninfected controls with little to no immune cell infiltrate (Fig. 4a, b).

We observed increased immune cell infiltrates in the brain of mice with neurotropic disease as compared with mice with viscerotropic disease (Fig. 4c, d), even though mice with viscerotropic disease had significantly higher viral titres in brain tissues (Fig. 3). These results suggested that the immune response to YFV-17D infection influenced pathology and disease outcome more than the amount of virus present.

Early indicators of disease outcome in IFNAR$^{-/-}$ mice

In order to determine if early indicators could predict eventual disease outcome we monitored weight changes and serum levels of a liver damage marker, alanine aminotransferase (ALT), in YFV-17D-infected mice. First, we measured the weights of uninfected 22-day-old IFNAR$^{-/-}$ mice and age-matched mice intramuscularly inoculated with 10^4 p.f.u. YFV-17D. We found that uninfected mice steadily gained weight, reaching 1.6 times their original weight at 30 days old (day 8 p.i.) (Fig. 5a). However, all YFV-17D-infected mice failed to gain weight starting at 5 days p.i. Mice that showed no clinical signs of disease maintained their weight, whilst mice that developed neurotropic disease or viscerotropic disease lost weight from 5 to 8 days p.i. At disease onset, mice with neurotropic and viscerotropic disease had significantly lower weights as compared with mice with no clinical signs of disease (Fig. 5a). However, at early times post-infection (days 1–5 p.i.), we could not discriminate between mice that would survive or succumb to YFV-17D infection. Second, we evaluated serum levels of ALT at 1, 3 and 5 days p.i. in mice that would eventually develop no clinical signs, neurotropic disease or viscerotropic disease. We found that at 1 and 3 days p.i., elevated ALT levels in mice correlated with the development of viscerotropic disease (Fig. 5b). We found that ALT levels were similar in all YFV-17D-infected mice at 5 days p.i. regardless of disease outcome (Fig. 5b). These results indicated that increased serum ALT levels at early time points after YFV-17D infection may precede development of viscerotropic disease.

YFV-17D infection of IFNAR$^{-/-}$ mice induces distinct chemokine/cytokine profiles

As we found increased immune infiltrates in the brains of mice with neurotropic disease and the amount of inflammatory infiltrate did not correlate with viral titres in the brain, we hypothesized that increased or improper cytokine induction contributed to distinct pathology and disease outcome in YFV-17D-infected IFNAR$^{-/-}$ mice. In humans, severe YFV infection has haemorrhagic manifestations associated with vascular permeability, which may be facilitated by cytokine induction (Monath, 2008; Paessler & Walker, 2013), and YFV infection of mice deficient for IFN-α/β and IFN-$\alpha/\beta/\gamma$ receptors induced high levels of proinflammatory cytokines (Meier et al., 2009; Thibodeaux et al., 2012). We initially evaluated cytokines at 5 days p.i.
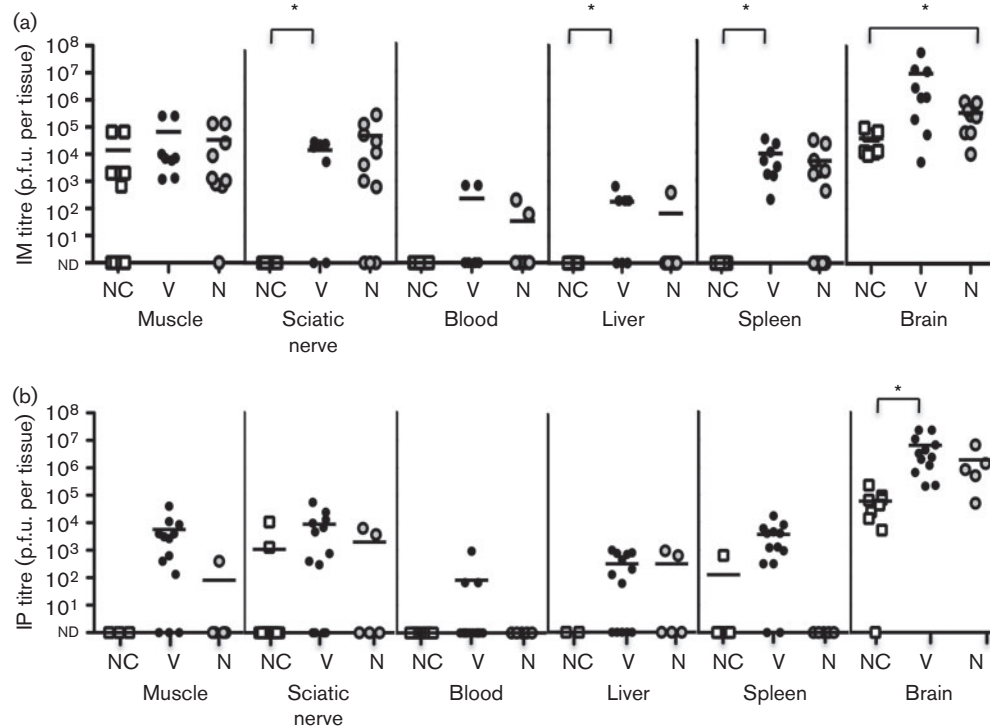
Fig. 3. YFV-17D tissue titres. IFNAR$^{-/-}$ mice were inoculated (a) intramuscularly (IM) or (b) intraperitoneally (IP) with 10^4 p.f.u. YFV-17D and tissues were harvested at disease onset (days 6–8 p.i.) for mice exhibiting viscerotropic (V) or neurotropic (N) disease, or day 8 p.i. for mice with no clinical signs of disease (NC). Viral titres were quantified using BHK-J cell plaque assays. Data are shown as p.f.u. per tissue, except for blood titres, which are shown as p.f.u. ml^{-1}. Results are from five to 20 mice per condition, with the mean indicated by a horizontal line. Differences that are statistically significant are shown by asterisks ($P < 0.05$, Student's t-test). ND, Titres below the detection limit of ~10 p.f.u. per tissue.

in serum samples from 3–4-week-old IFNAR$^{-/-}$ mice infected intramuscularly with 10^4 p.f.u. YFV-17D virus using the Mouse Cytokine Array Panel A kit (see Methods), which simultaneously profiled the relative levels of 40 cytokines. We compared samples from mice that were uninfected, mice that did not display clinical signs of disease and mice that eventually developed viscerotropic disease. Table S1 (available in the online Supplementary

Material) shows a complete list of the mean values obtained for each cytokine. Whilst levels of most cytokines were low or highly variable among groups of mice, we found that some cytokines, including IP-10 (also known as CXCL10) and MCP-1 (also known as JE or CCL2), were significantly increased in YFV-17D-infected mice with viscerotropic disease as compared with uninfected mice (Table S1, bold). Interestingly, these cytokines were also
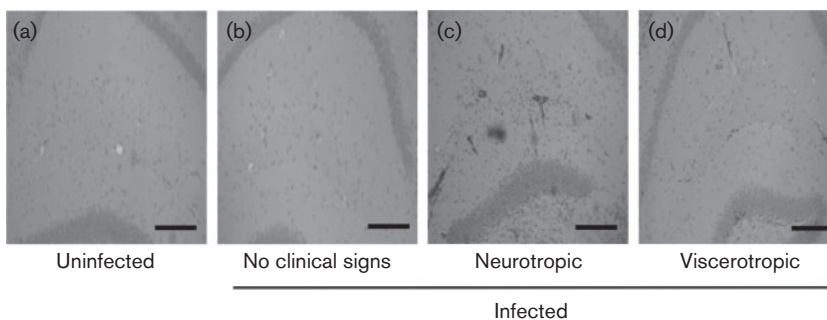

Fig. 4. Histology of brain tissue from YFV-17D-infected mice. IFNAR$^{-/-}$ mice were intramuscularly inoculated with 10^4 p.f.u. YFV-17D and brain tissue was harvested at disease onset (day 7 or 8 p.i.) for mice exhibiting viscerotropic or neurotropic disease, or day 8 p.i. for mice with no clinical signs of disease. Hippocampal sections from (a) uninfected, (b) no clinical signs, (c) neurotropic and (d) viscerotropic mice were histologically stained with HE. Immune infiltrates appear as dark clusters of cells. Sections are representative of at least two mice per condition. Bar, 100 µm.
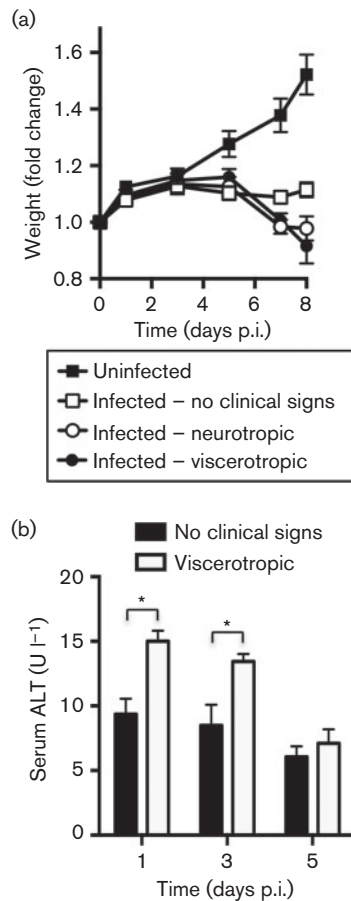
Fig. 5. Weight change and ALT levels in YFV-17D-infected mice. (a) IFNAR$^{-/-}$ mice (22 days old) were uninfected or intramuscularly inoculated with 10^4 p.f.u. YFV-17D. Fold changes in weight relative to initial weight were measured every other day until disease phenotype could be assigned. Results are shown as mean $\pm$ SEM from six to 20 mice per condition. Statistically significant differences were found between uninfected and infected mice from 5 to 8 days p.i., and between mice with no clinical signs and mice with neurotropic or viscerotropic disease at 7 or 8 days p.i. ($P<0.05$, Student's t-test). (b) Serum levels of ALT. IFNAR$^{-/-}$ mice (22 days old) were intramuscularly inoculated with 10^4 p.f.u. YFV-17D and at 1, 3 and 5 days p.i. serum samples were obtained and ALT levels measured using three to seven mice per group. Results are shown as mean $\pm$ SEM and are representative of two independent experiments. Statistically significant differences are indicated by asterisks ($P<0.05$, Student's t-test).

more highly induced in mice that developed viscerotropic disease as compared with infected animals displaying no clinical signs of disease.

To confirm the altered levels of IP-10 and MCP-1 in mice that developed viscerotropic disease, we used a standard sandwich ELISA to quantify cytokine levels in serum samples from IFNAR$^{-/-}$ mice intramuscularly infected with 10^4 p.f.u. YFV-17D at 5 days p.i. We found that IP-10 and MCP-1 were undetectable in uninfected mice (Fig. 6).
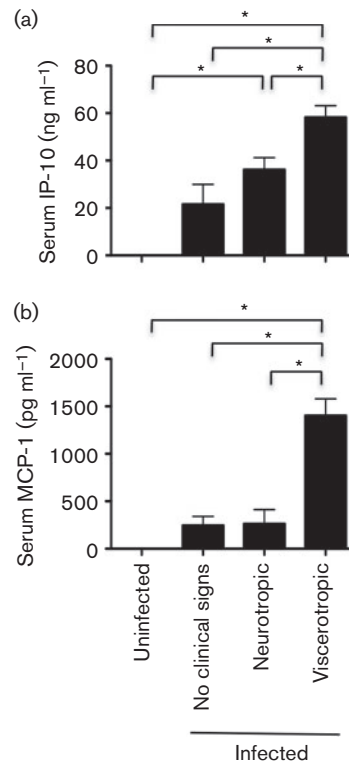

Fig. 6. IP-10 and MCP-1 levels in YFV-17D-infected mice. Serum levels of (a) IP-10 and (b) MCP-1 were measured in serum from uninfected IFNAR$^{-/-}$ mice and from IFNAR$^{-/-}$ mice intramuscularly inoculated with 10^4 p.f.u. YFV-17D. Serum was collected at 5 days p.i. and disease state was monitored through day 8 p.i., facilitating assignment of disease outcome. Results are shown as mean $\pm$ SEM with three mice per condition and are representative of three independent experiments. Statistically significant differences are indicated by asterisks ($P<0.05$, Student's t-test).

However, we found significantly elevated levels of IP-10 and MCP-1 in mice with viscerotropic disease as compared with infected mice showing no clinical signs of disease and mice with neurotropic disease (Fig. 6). These results suggested that high systemic induction of certain inflammatory cytokines may play a role in immunopathology during viscerotropic disease. Additionally, we found no significant differences in IP-10 and MCP-1 levels in the blood of mice with neurotropic disease compared with mice with no clinical signs of disease (Fig. 6), further supporting the idea that the specific host immune response contributed to pathology and disease outcome.

IP-10 influences YFV-17D pathogenesis in IFNAR$^{-/-}$ mice

Due to the high levels of IP-10 in mice with viscerotropic disease, we hypothesized that IP-10 contributed directly or indirectly to YFV-17D viscerotropic disease pathology. In order to determine if IP-10 influenced the pathogenesis of

YFV-17D, we intraperitoneally injected 3–4-week-old IFNAR$^{-/-}$ mice with PBS or 100 ng mouse recombinant IP-10 at −1, 1, 3 and 5 days p.i. with 10^7 p.f.u. YFV-17D and monitored mice daily for signs of disease. We found that significantly more mice succumbed to disease when treated with recombinant IP-10 and IP-10-treated mice developed disease sooner than PBS-treated mice (Fig. 7a). Additionally, 50 % of IP-10-treated mice developed viscerotropic disease, whereas only 17 % of PBS-treated mice developed viscerotropic disease (Fig. 7b). However, IP-10 treatment did not significantly alter the percentage of mice developing neurotropic disease (23 versus 14 %; $P>0.05$, χ^2 test). Therefore, IP-10 treatment increased YFV-17D pathogenesis by specifically enhancing viscerotropic disease.
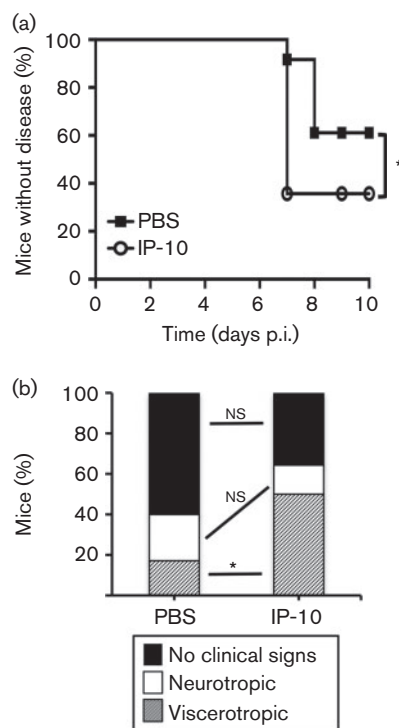

Fig. 7. Effect of recombinant IP-10 treatment on YFV-17D pathogenesis in mice. (a) Survival of YFV-17D-infected mice after treatment with IP-10. IFNAR$^{-/-}$ mice were intramuscularly inoculated with 10^7 p.f.u. YFV-17D and at −1, 1, 3 and 5 days p.i. 100 ng recombinant IP-10 or PBS was administered intraperitoneally. Disease onset was monitored and data are presented as the percentage without disease. Results are from 14 IP-10-treated mice and 35 PBS-treated mice. Statistically significant differences between survival of IP-10 and PBS-treated mice were found, indicated by an asterisk ($P<0.05$, Mantel–Cox test). (b) Percentages of mice displaying no clinical signs of disease, neurotropic disease or viscerotropic disease in YFV-17D-infected mice treated with PBS or IP-10. Statistically significant differences were observed between the percentages of mice with viscerotropic disease in the IP-10-treated group as compared with the PBS-treated group (50 versus 17 %, respectively; $P<0.001$, χ^2 test). NS, Not significant.

Together, our results suggested that IP-10 played a significant role in disease outcome in YFV-17D-infected IFNAR$^{-/-}$ mice.

DISCUSSION

In this study, we used YFV-17D infection of mice to examine factors that play a role in viral pathogenesis. We found that identically infected mice developed one of three distinct disease phenotypes: no clinical signs of disease, fatal viscerotropic disease or fatal neurotropic disease. We determined that the route of infection and host immune responses influenced YFV-17D pathogenesis more than the amount of virus.

In agreement with previous work, we found that YFV-17D was severely attenuated in immune-competent mice (Meier et al., 2009; Zisman et al., 1971). Similar to Meier et al. (2009), we found that subcutaneous inoculation of YFV-17D did not induce disease in IFNAR$^{-/-}$ mice. However, we found that infection with YFV-17D induced distinct neurotropic or viscerotropic disease in intramuscularly and intraperitoneally inoculated IFNAR$^{-/-}$ mice. These results confirm that inoculation route dramatically impacts disease outcome in YFV-17D-infected IFNAR$^{-/-}$ mice. Additionally, we found that a 1000-fold increase in virus inoculum did not illicit disease in immune-competent mice. Moreover, IFNAR$^{-/-}$ mice inoculated with 1000-fold more virus did not have significantly higher mortality rates and the percentage of mice with neurotropic versus viscerotropic disease was not changed, indicating that factors other than viral dose influenced disease outcome (Fig. 2). Similarly, DENV-induced paralysis in mice deficient for IFN-$\alpha/\beta/\gamma$ receptors was not largely impacted by viral inoculum dose (Prestwood et al., 2008). Ninety-one per cent of mice with viscerotropic disease had damage to visceral organs. To the best of our knowledge, ours is the first study to find YFV-17D-induced lethal viscerotropic disease in a mouse model (Fig. 1c–e, Table 1). Mice with neurotropic disease had increased immune cell infiltrates in the brain compared with mice with viscerotropic disease or no clinical signs of disease (Fig. 4). Similar immune cell infiltrates have been observed in hamsters and mice infected with YFV-17D, a neurovirulent DENV isolate, WNV and other neurotropic flaviviruses (Dominguez & Baruch, 1963; Hase et al., 1990; Klein et al., 2005; Liu & Chambers, 2001; Mateo et al., 2007; Wang et al., 2004).

Interestingly, a study of WT YFV infections in humans found similar levels of detectable YFV RNA in fatal haemorrhagic and non-fatal haemorrhagic cases (ter Meulen et al., 2004). Additionally, YFV-17D RNA was only detected in approximately half of patients with fatal YFV-AVD (Bae et al., 2008; Monath et al., 2013; ter Meulen et al., 2004). Similarly, we found that viral titres at disease onset did not correlate with disease outcome. For example, visceral tissue titres of mice with viscerotropic disease were not significantly higher than those in mice with neurotropic

disease and brain titres of mice with neurotropic disease were not significantly higher than those in mice with viscerotropic disease or no clinical signs of disease (Fig. 3). Mice with no clinical signs of disease recovered completely from infection despite having high viral titres in the central nervous system (Fig. 3). It is possible that immune deficiency due to lack of a type I IFN response facilitates robust viral replication in the brain, but that high viral titre alone does not promote disease. These results demonstrate that neuroinvasion does not always lead to disease, as has been noted after WNV infection of susceptible and resistant mouse strains (Brown *et al.*, 2007).

As viral titres at disease onset did not correlate with disease outcome, we examined cytokine profiles. In humans, severe DENV, YFV and YFV-17D-associated viscerotropic disease are potentially mediated by dysregulated secretion of cytokines and chemokines (Bae *et al.*, 2008; Lee *et al.*, 2006b; Monath, 2008; ter Meulen *et al.*, 2004). We found significantly elevated serum levels of IP-10 and MCP-1 in mice with viscerotropic disease as compared with mice with neurotropic disease and mice displaying no clinical signs of disease (Fig. 6). These results suggest that high levels of IP-10 and MCP-1 may promote viscerotropic disease. Other studies have found that MCP-1 and/or IP-10 levels correlated with disease severity during infection with viruses causing haemorrhagic fever, such as ebolavirus and hantavirus (Wang *et al.*, 2012; Wauquier *et al.*, 2010), as well as other flavivirus infections. MCP-1 levels were elevated in DENV-infected humans (Lee *et al.*, 2006a; Rathakrishnan *et al.*, 2012), severe YFV and YFV-17D infections in humans (Bae *et al.*, 2008; ter Meulen *et al.*, 2004), YFV-infected IFN-α/β and IFN-$\alpha/\beta/\gamma$ receptor knockout mice (Meier *et al.*, 2009; Thibodeaux *et al.*, 2012), and in some strains of WNV-infected mice (Kumar *et al.*, 2013). MCP-1 has previously been shown to increase vascular permeability and disrupt tight junctions in endothelial cells, suggesting a potential role in haemorrhagic manifestations and shock syndrome characteristic of fatal YFV and DENV infections (Lee *et al.*, 2006b; Rathakrishnan *et al.*, 2012).

Consistent with the idea that cytokines contribute to disease outcome, we found that administration of recombinant IP-10 during YFV-17D infection enhanced pathogenesis in IFNAR$^{-/-}$ mice, with significantly increased mortality rates and a higher percentage of mice that developed viscerotropic disease (Fig. 7). Elevated IP-10 levels have been associated with pathogenesis of numerous diseases (Liu *et al.*, 2011). IP-10 levels were significantly elevated in fatal as compared with non-fatal, non-haemorrhagic YFV human infections (ter Meulen *et al.*, 2004), YFV-17D-infected IFN-$\alpha/\beta/\gamma$ receptor knockout mice (Thibodeaux *et al.*, 2012), in DENV-infected mice and humans (Fink *et al.*, 2007; Rathakrishnan *et al.*, 2012; Sung *et al.*, 2012), in the spleen and brain tissues of WNV-infected mice (Shirato *et al.*, 2004), and correlated with liver damage in hepatitis C virus-infected patients (Liu *et al.*, 2011). It has been proposed that IP-10 could

promote haemorrhagic fever by affecting vascular permeability (Liu *et al.*, 2011). Interestingly, IP-10 was the only chemokine significantly induced in YFV-17D-vaccinated individuals (Querec *et al.*, 2009), suggesting an important role for YFV-17D immunogenicity in healthy humans with intact immune responses. It has also been shown that IP-10 contributes to decreased DENV replication in immune-deficient IFN regulatory factor (IRF)-3/ IRF-7 knockout mice (Chen *et al.*, 2013) and IP-10 reduces neurological disease in WNV- or DENV-infected mice (Hsieh *et al.*, 2006; Klein *et al.*, 2005). These findings suggest that chemokines and cytokines such as IP-10 play an important role in the balance between pathogen control and immunopathology, and these proteins may have different activity in neuronal versus non-neuronal tissues. Overall, elevated levels of proinflammatory cytokines such as IP-10 and MCP-1, and elevated levels of liver enzymes, may be better indicators of the severity of YFV and YFV-17D infection than viral titres.

In summary, we have demonstrated that various factors influence YFV-17D pathogenesis in immune-deficient mice. Overall, our results suggest that release of cytokines and chemokines by brain or visceral organs may induce tissue damage, leading to the distinct disease outcomes in YFV-17D-infected mice. Further investigation into the mechanisms that control viral disease outcome is warranted.

METHODS

Viruses and titre assay. Virus was produced by electroporation of YFV-17D RNA into BHK-J cells. Briefly, YFV-17D RNA was transcribed *in vitro* using a mMESSAGE mMACHINE SP6 kit (Ambion) according to the manufacturer's instructions and 1–5 μl of this *in vitro* transcription reaction was electroporated into ~10^7 BHK-J cells. A Gene Pulser Xcell electroporation system (Bio-Rad) was used with settings of 850 V, 5 ms pulse length, two pulses, 5 s pulse interval and 4 mm cuvette. BHK-J cells were grown in Dulbecco's modified Eagle's medium (DMEM) with 2 % FBS, plated on 10 cm dishes and 24–48 h later split into three 15 cm plates. Supernatant was harvested from 15 cm plates when cytopathic effect was detected. Viral titres were determined by adding serial dilutions of supernatant in serum-free medium to six-well plates containing ~10^6 BHK-J cells for 1 h. Supernatant was removed, cells washed and 5 ml agarose overlay containing 0.5 % SeaKem LE Agarose (Lonza) in DMEM containing 2 % FBS was added. After 5 days, agarose overlays were removed and cells were stained with an alcoholic crystal violet solution for plaque visualization.

Mouse experiments. All animals were handled in strict accordance with good animal practice as defined by the Guide for the Care and Use of Laboratory Animals of the National Institutes of Health. All mouse studies were performed at the University of Texas Southwestern Medical Center (Animal Welfare Assurance A3472-01) using protocols approved by the University of Texas Southwestern Institutional Animal Care and Use Committee (IACUC). All studies were performed in a manner designed to minimize pain and suffering, and any animals that exhibited severe disease signs were euthanized immediately in accordance with IACUC approved end points. For this study, WT mice were immune-competent C57BL/6 PVR-Tg21 mice (IFNAR$^{+/+}$) expressing the human poliovirus receptor and immune-deficient mice

were C57BL/6 PVR-Tg21 mice deficient for the IFN-α/β receptor (IFNAR$^{-/-}$) expressing the human poliovirus receptor (provided by S. Koike, Tokyo Metropolitan Institute of Medical Science, Tokyo, Japan) (Ida-Hosonuma et al., 2005). Mice (3–4 or 6–7 weeks old) were injected in the footpad, subcutaneously in the back scruff, intramuscularly in the left quadricep or intraperitoneally with 10^4 (Figs 1, 3, 4, 5 and 6) or 10^7 p.f.u. YFV-17D virus (Figs 2 and 7). Mice were monitored daily for signs of disease, as described in Results, and euthanized upon disease onset (6–8 days p.i.). As mice with severe disease do not recover from infection, we euthanized moribund mice and data are presented as the percentage of mice without disease. For evaluation of viral load at disease onset or 8 days p.i. in mice showing no clinical signs of disease, tissues from the inoculated quadricep muscle, whole sciatic nerve from the inoculated leg, brain, liver, spleen and blood were weighed and resuspended in 2–4 vols PBS and homogenized with a Bullet Blender tissue homogenizer (NextAdvance), as per the manufacturer's instructions. Tissue homogenates were then centrifuged at 13 000 r.p.m. for 1 min and supernatant virus stocks were used for viral titre assay as described above. For recombinant IP-10 experiments, 3–4-week-old IFNAR$^{-/-}$ mice were injected intraperitoneally with PBS or 100 ng recombinant mouse CXCL10/IP-10 (BioLegend) at −1, 1, 3 or 6 days followed by intramuscular injection with 10^7 p.f.u. YFV-17D on 'day 0'. Mice were monitored daily for signs of disease and euthanized upon disease onset (7–8 days p.i.).

Histological analysis. At disease onset (7–8 days p.i.), YFV-17D-infected mice with viscerotropic disease, neurotropic disease or no clinical signs and uninfected IFNAR$^{-/-}$ mice were given an intraperitoneal injection of a terminal dose of pentobarbital and were perfused with PBS/4 % paraformaldehyde, pH 7.4. Brains were post-fixed in PBS/4 % paraformaldehyde at 4 °C for 48 h and then sectioned via sagittal cuts with four sections per mouse. Subsequent paraffin processing, embedding, sectioning and HE staining were performed by standard procedures by the University of Texas Southwestern Pathology Core (Shehan & Barbara, 1980; Woods & Roy, 1996). Images were captured using a Zeiss Axiovert 200 microscope with an AxioCam MRm digital black and white camera.

Cytokine analysis. Serum samples from uninfected 3–4-week-old IFNAR$^{-/-}$ mice or IFNAR$^{-/-}$ mice intramuscularly inoculated with 10^4 p.f.u. YFV-17D were obtained using a 4 mm lancet and submandibular bleeding. Mice were observed until 8 days p.i. to determine eventual disease outcome. Blood samples were left at room temperature for 2 h, centrifuged for 20 min at 2000 *g*, and serum was collected and stored at −80 °C. The detection of cytokine levels in 20 µl serum samples was determined using the Mouse Cytokine Array Panel A (R&D Systems) according to the manufacturer's protocol. Membranes were exposed to X-ray film for 2 min, and the developed film was then scanned and pixel densities determined using ImageQuant image analysis software. Duplicate spots on each array were averaged and the background subtracted. The signals/pixel densities were then compared from each array representing an individual mouse, with two to three mice per condition. For measurement of ALT, IP-10 and MCP-1 levels in serum we used Single-Analyte ELISArray kits (MyBioSource, ALT; Qiagen, IP-10 and MCP-1) according to the manufacturer's protocol. Briefly, serum (20–60 µl) was diluted in sample dilution buffer to 300 µl and then 50 µl was added in duplicate to 96-well plates that were pre-coated with the target-specific capture antibody for each single protein. Additionally, a serial-diluted specific antigen standard was added to each plate in duplicate for determination of the standard curve. After 2 h the wells were washed and incubated with the detection antibody for 1 h, washed again and incubated with avidin-HRP for 30 min. Next, samples were incubated with the detection solution for 15 min. The stop solution was then added and the OD$_{450}$ was read immediately. Cytokine concentrations were calculated in each individual well based on the standard curve for duplicate samples from three to seven independent mice per disease phenotype.

REFERENCES

Anonymous (1966). Fatal viral encephalitis following 17D yellow fever vaccine inoculation. Report of a case in a 3-year-old child. *JAMA* **198**, 671–672.

Bae, H.-G., Domingo, C., Tenorio, A., de Ory, F., Muñoz, J., Weber, P., Teuwen, D. E. & Niedrig, M. (2008). Immune response during adverse events after 17D-derived yellow fever vaccination in Europe. *J Infect Dis* **197**, 1577–1584.

Barrett, A. D. & Gould, E. A. (1986). Comparison of neurovirulence of different strains of yellow fever virus in mice. *J Gen Virol* **67**, 631–637.

Beck, A., Tesh, R. B., Wood, T. G., Widen, S. G., Ryman, K. D. & Barrett, A. D. (2014). Comparison of the live attenuated yellow fever vaccine 17D-204 strain to its virulent parental strain Asibi by deep sequencing. *J Infect Dis* **209**, 334–344.

Belsher, J. L., Gay, P., Brinton, M., DellaValla, J., Ridenour, R., Lanciotti, R., Perelygin, A., Zaki, S., Paddock, C. & other authors (2007). Fatal multiorgan failure due to yellow fever vaccine-associated viscerotropic disease. *Vaccine* **25**, 8480–8485.

Brown, A. N., Kent, K. A., Bennett, C. J. & Bernard, K. A. (2007). Tissue tropism and neuroinvasion of West Nile virus do not differ for two mouse strains with different survival rates. *Virology* **368**, 422–430.

Card, J. P., Whealy, M. E., Robbins, A. K., Moore, R. Y. & Enquist, L. W. (1991). Two alpha-herpesvirus strains are transported differentially in the rodent visual system. *Neuron* **6**, 957–969.

Centers for Disease Control and Prevention (2002). Adverse events associated with 17D-derived yellow fever vaccination – United States, 2001–2002. *MMWR Morb Mortal Wkly Rep* **51**, 989–993.

Cetron, M. S., Marfin, A. A., Julian, K. G., Gubler, D. J., Sharp, D. J., Barwick, R. S., Weld, L. H., Chen, R., Clover, R. D. & other authors (2002). Yellow fever vaccine. Recommendations of the Advisory Committee on Immunization Practices (ACIP), 2002. *MMWR Recomm Rep* **51** (RR-17), 1–11.

Chan, R. C., Penney, D. J., Little, D., Carter, I. W., Roberts, J. A. & Rawlinson, W. D. (2001). Hepatitis and death following vaccination with 17D-204 yellow fever vaccine. *Lancet* **358**, 121–122.

Chen, H. W., King, K., Tu, J., Sanchez, M., Luster, A. D. & Shresta, S. (2013). The roles of IRF-3 and IRF-7 in innate antiviral immunity against dengue virus. *J Immunol* **191**, 4194–4201.

Dominguez, A. & Baruch, E. (1963). Histopathology of the central nervous system in Swiss mice intracerebrally inoculated with 17-D strain of yellow fever virus. *Am J Trop Med Hyg* **12**, 815–819.

Erickson, A. K. & Pfeiffer, J. K. (2013). Dynamic viral dissemination in mice infected with yellow fever virus strain 17D. *J Virol* **87**, 12392–12397.

Fink, J., Gu, F., Ling, L., Tolfvenstam, T., Olfat, F., Chin, K. C., Aw, P., George, J., Kuznetsov, V. A. & other authors (2007). Host gene expression profiling of dengue virus infection in cell lines and patients. *PLoS Negl Trop Dis* 1, e86.

Fitzgeorge, R. & Bradish, C. J. (1980). The *in vivo* differentiation of strains of yellow fever virus in mice. *J Gen Virol* 46, 1–13.

Fox, J. P. (1943). Immunity to yellow fever encephalitis of monkeys and mice immunized by neural and extraneural routes. *J Exp Med* 77, 487–506.

Gerasimon, G. & Lowry, K. (2005). Rare case of fatal yellow fever vaccine-associated viscerotropic disease. *South Med J* 98, 653–656.

Goodman, G. T. & Koprowski, H. (1962). Macrophages as a cellular expression of inherited natural resistance. *Proc Natl Acad Sci U S A* 48, 160–165.

Guirakhoo, F., Kitchener, S., Morrison, D., Forrat, R., McCarthy, K., Nichols, R., Yoksan, S., Duan, X., Ermak, T. H. & other authors (2006). Live attenuated chimeric yellow fever dengue type 2 (ChimeriVax-DEN2) vaccine: Phase I clinical trial for safety and immunogenicity: effect of yellow fever pre-immunity in induction of cross neutralizing antibody responses to all 4 dengue serotypes. *Hum Vaccin* 2, 60–67.

Guy, B., Guirakhoo, F., Barban, V., Higgs, S., Monath, T. P. & Lang, J. (2010). Preclinical and clinical development of YFV 17D-based chimeric vaccines against dengue, West Nile and Japanese encephalitis viruses. *Vaccine* 28, 632–649.

Hahn, C. S., Dalrymple, J. M., Strauss, J. H. & Rice, C. M. (1987). Comparison of the virulent Asibi strain of yellow fever virus with the 17D vaccine strain derived from it. *Proc Natl Acad Sci U S A* 84, 2019–2023.

Hase, T., Dubois, D. R. & Summers, P. L. (1990). Comparative study of mouse brains infected with Japanese encephalitis virus by intracerebral or intraperitoneal inoculation. *Int J Exp Pathol* 71, 857–869.

Horsfall, F. L. & Tam, I. (editors) (1965). *Viral and Rickettsial Infections of Man*, 4th edn. Philadelphia, PA: Lippincott.

Hsieh, M. F., Lai, S. L., Chen, J. P., Sung, J. M., Lin, Y. L., Wu-Hsieh, B. A., Gerard, C., Luster, A. & Liao, F. (2006). Both CXCR3 and CXCL10/IFN-inducible protein 10 are required for resistance to primary infection by dengue virus. *J Immunol* 177, 1855–1863.

Ida-Hosonuma, M., Iwasaki, T., Yoshikawa, T., Nagata, N., Sato, Y., Sata, T., Yoneyama, M., Fujita, T., Taya, C. & other authors (2005). The alpha/beta interferon response controls tissue tropism and pathogenicity of poliovirus. *J Virol* 79, 4460–4469.

Kengsakul, K., Sathirapongsasuti, K. & Punyagupta, S. (2002). Fatal myeloencephalitis following yellow fever vaccination in a case with HIV infection. *J Med Assoc Thai* 85, 131–134.

Khaiboullina, S. F., Rizvanov, A. A., Holbrook, M. R. & St Jeor, S. (2005). Yellow fever virus strains Asibi and 17D-204 infect human umbilical cord endothelial cells and induce novel changes in gene expression. *Virology* 342, 167–176.

Klein, R. S., Lin, E., Zhang, B., Luster, A. D., Tollett, J., Samuel, M. A., Engle, M. & Diamond, M. S. (2005). Neuronal CXCL10 directs CD8^{+} T-cell recruitment and control of West Nile virus encephalitis. *J Virol* 79, 11457–11466.

Kumar, M., Roe, K., Orillo, B., Muruve, D. A., Nerurkar, V. R., Gale, M., Jr & Verma, S. (2013). Inflammasome adaptor protein Apoptosis-associated speck-like protein containing CARD (ASC) is critical for the immune response and survival in West Nile virus encephalitis. *J Virol* 87, 3655–3667.

Lee, E. & Lobigs, M. (2008). E protein domain III determinants of yellow fever virus 17D vaccine strain enhance binding to glycosaminoglycans, impede virus spread, and attenuate virulence. *J Virol* 82, 6024–6033.

Lee, E., Wright, P. J., Davidson, A. & Lobigs, M. (2006a). Virulence attenuation of Dengue virus due to augmented glycosaminoglycan-binding affinity and restriction in extraneural dissemination. *J Gen Virol* 87, 2791–2801.

Lee, Y. R., Liu, M. T., Lei, H. Y., Liu, C. C., Wu, J. M., Tung, Y. C., Lin, Y. S., Yeh, T. M., Chen, S. H. & Liu, H. S. (2006b). MCP-1, a highly expressed chemokine in dengue haemorrhagic fever/dengue shock syndrome patients, may cause permeability change, possibly through reduced tight junctions of vascular endothelium cells. *J Gen Virol* 87, 3623–3630.

Liprandi, F. & Walder, R. (1983). Replication of virulent and attenuated strains of yellow fever virus in human monocytes and macrophage-like cells (U937). *Arch Virol* 76, 51–61.

Liu, T. & Chambers, T. J. (2001). Yellow fever virus encephalitis: properties of the brain-associated T-cell response during virus clearance in normal and gamma interferon-deficient mice and requirement for CD4^{+} lymphocytes. *J Virol* 75, 2107–2118.

Liu, M., Guo, S., Hibbert, J. M., Jain, V., Singh, N., Wilson, N. O. & Stiles, J. K. (2011). CXCL10/IP-10 in infectious diseases pathogenesis and potential therapeutic implications. *Cytokine Growth Factor Rev* 22, 121–130.

Martin, M., Tsai, T. F., Cropp, B., Chang, G. J., Holmes, D. A., Tseng, J., Shieh, W., Zaki, S. R., Al-Sanouri, I. & other authors (2001). Fever and multisystem organ failure associated with 17D-204 yellow fever vaccination: a report of four cases. *Lancet* 358, 98–104.

Mateo, R. I., Xiao, S. Y., Travassos da Rosa, A. P., Lei, H., Guzman, H., Lu, L. & Tesh, R. B. (2007). Yellow fever 17-D vaccine is neurotropic and produces encephalitis in immunosuppressed hamsters. *Am J Trop Med Hyg* 77, 919–924.

Meier, K. C., Gardner, C. L., Khoretonenko, M. V., Klimstra, W. B. & Ryman, K. D. (2009). A mouse model for studying viscerotropic disease caused by yellow fever virus infection. *PLoS Pathog* 5, e1000614.

Monath, T. P. (2008). Treatment of yellow fever. *Antiviral Res* 78, 116–124.

Monath, T. P. & Barrett, A. D. (2003). Pathogenesis and pathophysiology of yellow fever. *Adv Virus Res* 60, 343–395.

Monath, T. P., Guirakhoo, F., Nichols, R., Yoksan, S., Schrader, R., Murphy, C., Blum, P., Woodward, S., McCarthy, K. & other authors (2003). Chimeric live, attenuated vaccine against Japanese encephalitis (ChimeriVax-JE): phase 2 clinical trials for safety and immunogenicity, effect of vaccine dose and schedule, and memory response to challenge with inactivated Japanese encephalitis antigen. *J Infect Dis* 188, 1213–1230.

Monath, T. P., Liu, J., Kanesa-Thasan, N., Myers, G. A., Nichols, R., Deary, A., McCarthy, K., Johnson, C., Ermak, T. & other authors (2006). A live, attenuated recombinant West Nile virus vaccine. *Proc Natl Acad Sci U S A* 103, 6694–6699.

Monath, T. P., Gershman, M., Staples, J. E. & Barrett, A. D. (2013). Yellow fever vaccine. In *Vaccines*, 6th edn, pp. 870–968. Edited by S. A. Plotkin, W. Orenstein & P. A. Offit. London: Saunders.

Ohka, S., Yang, W. X., Terada, E., Iwasaki, K. & Nomoto, A. (1998). Retrograde transport of intact poliovirus through the axon via the fast transport system. *Virology* 250, 67–75.

Paessler, S. & Walker, D. H. (2013). Pathogenesis of the viral hemorrhagic fevers. *Annu Rev Pathol* 8, 411–440.

Prestwood, T. R., Prigozhin, D. M., Sharar, K. L., Zellweger, R. M. & Shresta, S. (2008). A mouse-passaged dengue virus strain with reduced affinity for heparan sulfate causes severe disease in mice by establishing increased systemic viral loads. *J Virol* 82, 8411–8421.

Pugachev, K. V., Guirakhoo, F. & Monath, T. P. (2005). New developments in flavivirus vaccines with special attention to yellow fever. *Curr Opin Infect Dis* 18, 387–394.

Querec, T. D., Akondy, R. S., Lee, E. K., Cao, W., Nakaya, H. I., Teuwen, D., Pirani, A., Gernert, K., Deng, J. & other authors (2009). Systems biology approach predicts immunogenicity of the yellow fever vaccine in humans. *Nat Immunol* **10**, 116–125.

Rathakrishnan, A., Wang, S. M., Hu, Y., Khan, A. M., Ponnampalavanar, S., Lum, L. C., Manikam, R. & Sekaran, S. D. (2012). Cytokine expression profile of dengue patients at different phases of illness. *PLoS One* **7**, e52215.

Samuel, M. A., Wang, H., Siddharthan, V., Morrey, J. D. & Diamond, M. S. (2007). Axonal transport mediates West Nile virus entry into the central nervous system and induces acute flaccid paralysis. *Proc Natl Acad Sci U S A* **104**, 17140–17145.

Schlesinger, J. J. & Brandriss, M. W. (1981). Antibody-mediated infection of macrophages and macrophage-like cell lines with 17D-yellow fever virus. *J Med Virol* **8**, 103–117.

Sellards, A. W. (1931). The behavior of the virus of yellow fever in monkeys and mice. *Proc Natl Acad Sci U S A* **17**, 339–343.

Shehan, D. C. H. & Barbara, B. (1980). *Theory and Practice of Histotechnology*, 2nd edn. Columbus, OH: Battelle Press.

Shirato, K., Kimura, T., Mizutani, T., Kariwa, H. & Takashima, I. (2004). Different chemokine expression in lethal and non-lethal murine West Nile virus infection. *J Med Virol* **74**, 507–513.

Silva, M. L., Espírito-Santo, L. R., Martins, M. A., Silveira-Lemos, D., Peruhype-Magalhães, V., Caminha, R. C., de Andrade Maranhão-Filho, P., Auxiliadora-Martins, M., de Menezes Martins, R. & other authors (2010). Clinical and immunological insights on severe, adverse neurotropic and viscerotropic disease following 17D yellow fever vaccination. *Clin Vaccine Immunol* **17**, 118–126.

Sung, J. M., Lee, C. K. & Wu-Hsieh, B. A. (2012). Intrahepatic infiltrating NK and CD8 T cells cause liver cell death in different phases of dengue virus infection. *PLoS One* **7**, e46292.

ter Meulen, J., Sakho, M., Koulemou, K., Magassouba, N., Bah, A., Preiser, W., Daffis, S., Klewitz, C., Bae, H. G. & other authors (2004). Activation of the cytokine network and unfavorable outcome in patients with yellow fever. *J Infect Dis* **190**, 1821–1827.

Theiler, M. (1930). Susceptibility of white mice to the virus of yellow fever. *Science* **71**, 367.

Thibodeaux, B. A., Garbino, N. C., Liss, N. M., Piper, J., Blair, C. D. & Roehrig, J. T. (2012). A small animal peripheral challenge model of yellow fever using interferon-receptor deficient mice and the 17D-204 vaccine strain. *Vaccine* **30**, 3180–3187.

Tyler, K. L., McPhee, D. A. & Fields, B. N. (1986). Distinct pathways of viral spread in the host determined by reovirus S1 gene segment. *Science* **233**, 770–774.

Vasconcelos, P. F., Luna, E. J., Galler, R., Silva, L. J., Coimbra, T. L., Barros, V. L., Monath, T. P., Rodrigues, S. G., Laval, C. & other authors (2001). Serious adverse events associated with yellow fever 17DD vaccine in Brazil: a report of two cases. *Lancet* **358**, 91–97.

Wang, T., Town, T., Alexopoulou, L., Anderson, J. F., Fikrig, E. & Flavell, R. A. (2004). Toll-like receptor 3 mediates West Nile virus entry into the brain causing lethal encephalitis. *Nat Med* **10**, 1366–1373.

Wang, P. Z., Li, Z. D., Yu, H. T., Zhang, Y., Wang, W., Jiang, W. & Bai, X. F. (2012). Elevated serum concentrations of inflammatory cytokines and chemokines in patients with haemorrhagic fever with renal syndrome. *J Int Med Res* **40**, 648–656.

Wauquier, N., Becquart, P., Padilla, C., Baize, S. & Leroy, E. M. (2010). Human fatal Zaire ebola virus infection is associated with an aberrant innate immunity and with massive lymphocyte apoptosis. *PLoS Negl Trop Dis* **4**, e837.

Woods, A.E. & Roy, C. (1996). *Laboratory Histopathology: A Complete Reference*. London: Churchill Livingston.

Zisman, B., Wheelock, E. F. & Allison, A. C. (1971). Role of macrophages and antibody in resistance of mice against yellow fever virus. *J Immunol* **107**, 236–243.